

Hirshfeld Surface Analysis of a Zn(II) Polymer¹

J. Wang^{a,*}, X. R. Wu^{b, **}, W. P. Wu^a, J. Q. Liu^b, and A. Kumar^{c, ***}

^a Institute of Functionalized Materials, Sichuan University of Science & Engineering, Zigong, 643000 P.R. China and School of Chemistry and Pharmaceutical Engineering, Sichuan University of Science & Engineering, Zigong 643000, P.R. China

^b School of Pharmacy, Guangdong Medical College, Dongguan, 523808 P.R. China

^c Department of Chemistry, University of Lucknow, Lucknow, 226007 India

e-mail: scwangjun2011@126.com*; xirenwu@163.com**; kumar_abhinav@lkouniv.ac.in***

Received October 1, 2014

Abstract—A new Zn-based complex with oxalate, namely $[\text{NH}_2(\text{CH}_3)_2][\text{Zn}(\text{Ox})_{1.5}] \cdot \text{DMF} \cdot \text{H}_2\text{O}$ (**I**) (Ox = oxalate), has been synthesized and structurally characterized. Single-crystal X-ray analysis of compound **I** reveals that the Ox ligand links the Zn(II) center, generating an intricate 2D classical honeycomb-like architecture (CIF file CCDC no. 1028787). The detail analyses of Hirshfeld surface and fingerprint plots gave a mode of non-covalent interactions in the title compound.

DOI: 10.1134/S1070328415050085

INTRODUCTION

The main goal of crystal engineering is to realize the intermolecular interactions in the context of crystal packing toward the design and synthesis of functional materials [1–5]. Aakeröy and Beatty said that predicting and controlling the competition between intermolecular forces are part of every crystal engineering effort [6]. Thus, how do we unravel the bundle of often inter-related interactions and identify strong, directional, reliable non-covalent interactions [7–9].

In the last few years the analysis of molecular crystal structures using tools based on Hirshfeld surfaces has rapidly gained in popularity. Hirshfeld surfaces were named after F.L. Hirshfeld, whose “stockholder partitioning” scheme for defining atoms in molecules suggested to us an extension to defining a molecule in a crystal [10]. This approach represents an attempt to venture beyond the current paradigm-internuclear distances and angles, crystal packing diagrams with molecules represented via various models [11, 12].

Molecular Hirshfeld surfaces [13] in the crystal structure were constructed on the basis of the electron distribution calculated as the sum of spherical atom electron densities [14, 15]. For a given crystal structure and a set of spherical atomic densities, the Hirshfeld surface is unique [16]. The normalized contact distance (d_{norm}) based on both d_e and d_i (where d_e is distance from a point on the surface to the nearest nucleus outside the surface and d_i is distance from a point on the surface to the nearest nucleus inside the surface) and the van der Waals (vdW) radii of the atom, as given by Eq. (1) enables identification of the regions of particular importance to intermolecular interactions. The combination of d_e and d_i in the form of two-dimen-

sional (2D) fingerprint plot [17, 18] provides a summary of intermolecular contacts in the crystal [13]. The Hirshfeld surfaces mapped with d_{norm} and 2D fingerprint plots were generated using the Crystal-Explorer 2.1 [19]. Graphical plots of the molecular Hirshfeld surfaces mapped with d_{norm} used a red-white-blue colour scheme, where red highlight shorter contacts, white represents the contact around van der Waals separation, and blue is for longer contact. Additionally, two further coloured plots representing shape index and curvedness based on local curvatures are also presented in this paper [20]

$$d_{\text{norm}} = \frac{d_i - r_i^{\text{vdW}}}{r_i^{\text{vdW}}} + \frac{d_e - r_e^{\text{vdW}}}{r_e^{\text{vdW}}}. \quad (1)$$

In this work, we prepared a new complex of $[\text{NH}_2(\text{CH}_3)_2][\text{Zn}(\text{Ox})_{1.5}] \cdot \text{DMF} \cdot \text{H}_2\text{O}$ (**I**) (Ox = oxalate), which shows an intricate 2D classical honeycomb-like architecture. Furthermore, we concern on the detail analyses of Hirshfeld surface and fingerprint plots of **I**.

EXPERIMENTAL

Materials and methods. All reagents were purchased from commercial sources and used as received. Thermogravimetric analyses (TGA) were carried out with a Metter–Toledo TA 50 in dry dinitrogen (60 mL min⁻¹) at a heating rate of 5°C min⁻¹.

Synthesis of I. A mixture of $\text{Zn}(\text{OAc})_2$ (0.1 mmol), 1,3,5-benzenetribenzoic acid (H_3Btb) (0.1 mmol), DMF (8 mL) and HNO_3 (0.1 mL) was placed in a vial, heated to 105°C for 3 days under autogenous pressure, and then cooled to room temperature at a rate of 5°C/h. Colorless crystals were obtained after 4 days.

¹ The article is published in the original.

Crystallographic data and structure refinement details for complex **I**

Parameter	Value
F_w	197.40
Crystal system	Trigonal
Space group	$P-32$
$a, \text{\AA}$	9.379(2)
$b, \text{\AA}$	9.379(2)
$c, \text{\AA}$	8.216(2)
$V, \text{\AA}^3$	625.9(3)
$\rho_{\text{calcd}}, \text{g cm}^{-3}$	1.047
Z	2
μ, mm^{-1}	1.946
$F(000)$	192
θ Range, deg	2.12–25.68
Index ranges hkl	$-5 \leq h \leq 13,$ $-10 \leq k \leq 12,$ $-11 \leq l \leq 9$
Reflections collected	2658
Independent reflections	692
R_{int}	0.0395
Reflections with $I > 2\sigma(I)$	376
GOOF	1.050
$R_1, wR_2 (I > 2\sigma(I))$	0.0440, 0.1184
R_1, wR_2 (all data)	0.0825, 0.1442
$\Delta\rho_{\text{max}}/\Delta\rho_{\text{min}}, e \text{\AA}^{-3}$	0.406/−0.291

The resulting crystals formed were filtered off, washed with water and dried in air. The yeild was 35% based on Zn.

For $\text{C}_8\text{H}_{17}\text{N}_2\text{O}_7\text{Zn}$

anal. calcd., %: C, 30.16; H, 5.38; N, 8.80.
Found, %: C, 30.20; H, 5.30; N, 8.79.

X-ray crystallography. Single crystal X-ray diffraction analysis of the compound was carried out on a Bruker SMART APEX II CCD diffractometer equipped with graphite monochromated MoK_α radiation ($\lambda = 0.71073 \text{\AA}$) by using $\omega-\varphi$ scan technique at room temperature. The intensities were corrected for Lorentz and polarization effects as well as for empirical absorption based on multi-scan techniques; the structures was solved by direct methods and refined by full-matrix least-squares fitting on F^2 using SHEXL-97 [21]. Absorption corrections were applied using the multi-scan approach with the program SADABS [22]. The hydrogen atoms of the organic ligands were placed in calculated positions and refined using a riding model

on attached atoms with isotropic thermal parameters 1.2 times those of their carrier atoms. Large sections of the structure consist of void space filled with disordered solvate molecules and counter cations. The dimethyl ammonium cation was generated from decomposition of dimethyl formamide. Indeed, the unit cell volume includes a region of disordered DMF and water molecules which could not be modeled as well discrete atomic sites, but their compositions can be confirmed by elemental analysis data, and TGA. Thus, they are included in the final formula. Table shows crystallographic data of **I**.

Supplementary material has been deposited with the Cambridge Crystallographic Data Centre (CCDC no. 1028787; deposit@ccdc.cam.ac.uk or <http://www.ccdc.cam.ac.uk>).

RESULTS AND DISCUSSION

X-ray crystallography reveals that in the asymmetric unit of **I**, each Zn(II) atom is six-coordinated by three oxygen atoms from four high symmetric Ox ligands and exhibits a slightly distorted tetrahedral geometry ($\text{Zn}(1)-\text{O}(1)^{\#1} 12.086(2) \text{\AA}$, $\text{O}(1)\text{Zn}(1)\text{O}(1)^{\#1} 168.92(11)^\circ$; $^{\#1} -x, -y, -z$). (Fig. 1). The Ox and $\text{H}_2(\text{CH}_3)_2$ are also generated from DMF molecule under acid catalysis. In this crystal, the Zn(II) centers are polymerized through the Ox units to yield two-dimensional layer with hexagonal pore along the xz plane (Fig. 2). The free DMF and cation hold at the empty hexagonal cavity with adimension of $10.8(7) \text{\AA}$ edge distances (Fig. 2).

The Hirshfeld surfaces of title compound are illustrated in Fig. 3, showing surfaces that have been mapped over a d_{norm} range of -0.5 to 1.5\AA , shape index (-1.0 to 1.0\AA) and curvedness (-4.0 to 0.4\AA). The surfaces are shown as transparent to allow visualization of the cavities and the potential donors and acceptors around which they were calculated. The weak interaction information discussed in X-ray crystallography section is summarized effectively in the spots, with the large circular depressions (deep red) visible on the d_{norm} surfaces indicative of hydrogen bonding contacts. The dominant interactions for the compound can be seen in Hirshfeld surface plots as the bright red shaded area in Fig. 3.

The fingerprint plots for Zinc oxalate cluster compound are presented in Fig. 4. The C–O interactions appear as two distinct spikes of almost equal lengths in the 2D fingerprint plots in the region $2.03 \text{\AA} < (d_e + d_i) < 2.47 \text{\AA}$ as light sky-blue pattern in full fingerprint 2D plots. Complementary regions are visible in the fingerprint plots where one molecule acts as a donor ($d_e > d_i$) and the other as an acceptor ($d_e < d_i$). The fingerprint plots can be decomposed to highlight particular atom pair close contacts. This decomposition enables separation of contributions from different interaction types, which overlap in the full fingerprint. The proportions of interactions contain 13.4% Hirshfeld surface from the full motif.

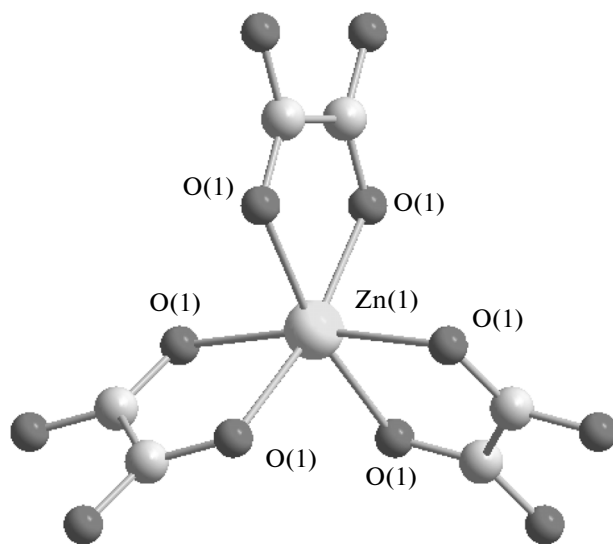


Fig. 1. View of the coordination environment of Zn(II) center in **I**.

To study the stability of the polymer, TGA of complex **I** was performed (Fig. 5). The compound **I** shows two of weight loss steps. The first weight loss began at 51°C and completed at 287°C. The observed weight loss of 28.1% is corresponding to the loss of the free DMF and H₂O molecules (calcd. 27.3%). The second weight loss occurs in the range 356–415°C, which can be attributed to the elimination of organic Ox and

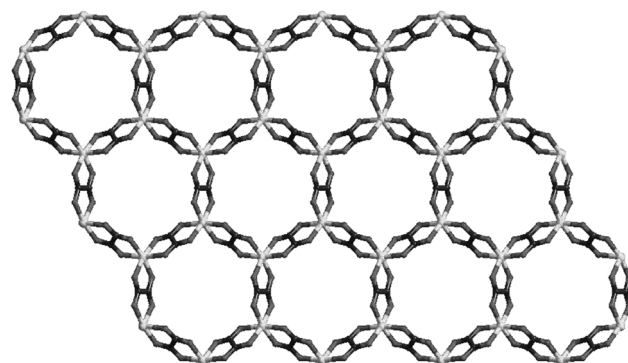


Fig. 2. Perspective view 2D net in **I**.

Me₂NH₂. The 20.5% mass remnant at 680°C is consistent with ZnO (21.1% predicted).

Thus, we have successfully synthesized one new polymer, which shows an intricate 2D classical honeycomb-like architecture. The detail analyses of Hirshfeld surface and fingerprint plots gave a mode of non-covalent interactions in the title compound.

ACKNOWLEDGMENTS

This work was partially supported by the Grants from Sichuan University of Science and Engineering, the Institute of Functionalized Materials (grant nos. 2012KY12 and 2014PY01), the Opening Project of Key Laboratory of Green Catalysis of Sichuan In-

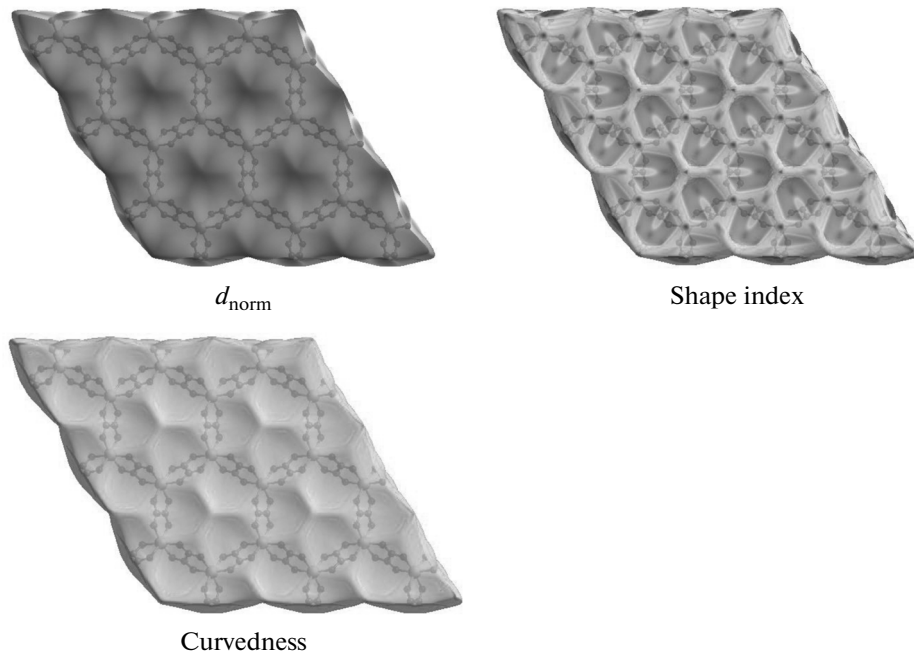


Fig. 3. Hirshfeld surfaces mapped with d_{norm} ; shape index, and curvedness for **I**.

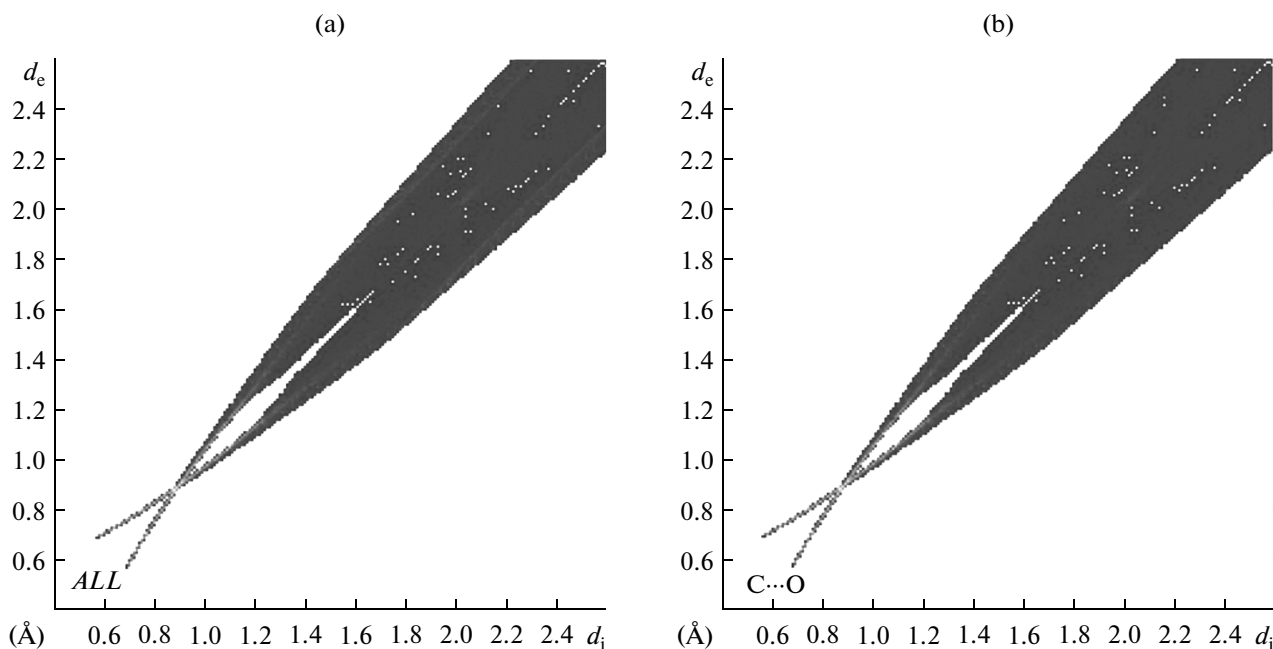


Fig. 4. Fingerprint plots Full (a), resolved into C···O (b) for the I.

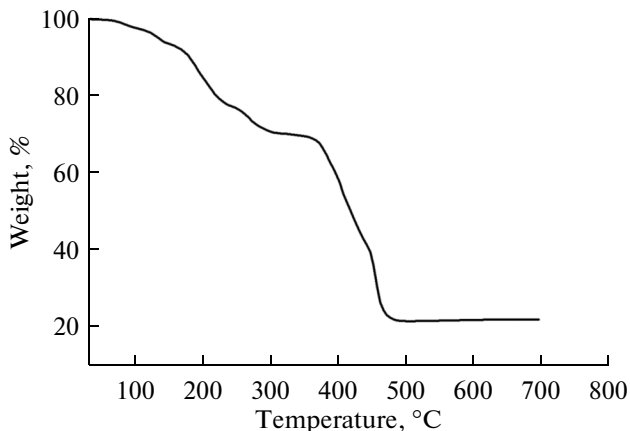


Fig. 5. View of the TGA in I.

stitutes of High Education (no. LYJ1207), and the Education Committee of Sichuan Province (nos. 12ZA090, 13ZB0131 and 14ZB0220) and thanks to Dr. M. Zeller.

REFERENCES

1. Spackman, M.A. and Jayatilaka, D., *CrystEngComm*, 2009, vol. 11, p. 19.
2. Desiraju, G.R., *Crystal Engineering: The Design of Organic Solids*, Amsterdam: Elsevier, 1989.
3. Allen, F.H., *Acta Crystallogr., B*, 2002, vol. 58, p. 380.
4. Desiraju, G.R., *Chem. Commun.*, 1997, p. 1475.
5. Aakeröy, C.B., Beatty, A.M., Tremayne, M.D., et al., *Cryst. Growth Des.*, 2001, vol. 1, p. 377.
6. Aakeröy, C.B. and Beatty, A.M., *Aust. J. Chem.*, 2001, vol. 54, p. 409.
7. Scheiner, S., *Hydrogen Bonding: A Theoretical Perspective*, Oxford (UK): Oxford Univ. Press, 1997.
8. Farrugia, L.J.J., *Appl. Crystallogr.*, 1997, vol. 30, p. 565.
9. Favre-Nicolin, V. and Cerny, R.J., *Appl. Crystallogr.*, 2002, vol. 35, p. 734. <http://objcryst.sourceforge.net>
10. Hirshfeld, F.L., *Theor. Chim. Acta*, 1977, vol. 44, p. 129.
11. Spackman, M.A. and Byrom P.G., *Chem. Phys. Lett.*, 1997, vol. 267, p. 215.
12. Dalapati, S., Saha, R., Jana, S., et al., *Angew. Chem. Int. Ed.*, 2012, vol. 51, p. 12534.
13. Spackman, M.A. and McKinnon, J.J., *CrystEngComm*, 2002, vol. 4, p. 378.
14. Spackman, M.A. and Byrom, P.G., *Chem. Phys. Lett.*, 1997, vol. 267, p. 309.
15. McKinnon, J.J., Mitchell, A.S., and Spackman, M.A., *Chem. Eur. J.*, 1998, vol. 4, p. 2136.
16. McKinnon, J.J., Spackman, M.A., and Mitchell, A.S., *Acta Crystallogr., B*, 2004, vol. 60, p. 627.
17. Rohl, A.L., Moret, M., Kaminsky, W., et al., *Cryst. Growth Des.*, 2008, vol. 8, p. 4517.
18. Parkin, A., Barr, G., Dong, W., et al., *CrystEngComm*, 2007, vol. 9, p. 648.
19. Wolff, S.K., Greenwood, D.J., McKinnon, J.J., et al., *Crystal Explorer 2.0*, Perth (Australia): Univ. of Western Australia, 2007.
20. Koenderink, J.J. and van Doorn, A.J., *Image Vision Comput.*, 1992, vol. 10, p. 557.
21. Sheldrick, G.M., *SHELXL-97, Program for Structure Determination and Refinement*, Göttingen (Germany): Univ. of Göttingen, 1997.
22. Sheldrick, G.M., *Acta Crystallogr. A*, 2008, vol. 64, p. 112.